Discussion Paper No.309

Delay Growth Model augmented with Physical and Human Capitals

Akio Matsumoto
Chuo University

Ferenc Szidarovszky
Corvinus University

March 2019

INSTITUTE OF ECONOMIC RESEARCH
Chuo University
Tokyo, Japan

Delay Growth Model augmented with Physical and Human Capitals*

Akio Matsumoto[†] Ferenc Szidarovszky[‡]

Abstract

A growth model augmented with physical capital and human capital is modified and used to explain the birth of cyclical dynamics. Crucial feature of the model is the assumption that there are a gestation delay and a maturation delay in constructing physical capital and human capital, respectively. Dynamics is described by a continuous time system of delay differential equations. A stability switching curve is analytically derived on which stability of the model is lost. Its shape is numerically verified and it is confirmed that the two-delay model can generate a wide variety of dynamics from simple dynamics to complex dynamics.

*The first author highly acknowledges the financial supports from the Japan Society for the Promotion of Science (Grant-in-Aid for Scientific Research (C) 16K03556) and Chuo University (Grant for Special Research). The usual disclaimers apply.

†Professor, Department of Economics, Chuo University, 742-1, Higashi-Nakano, Hachioji, Tokyo, 192-0393, Japan; akiom@tamacc.chuo-u.ac.jp

‡Professor, Department of Mathematics, Corvinus University, Budapest, Fövám tèr 8, H-1093, Hungary, szidarka@gmail.com

1 Introduction

It has been well-known by economists that wine is not made in a day. It is also well-known that economic models usually assume instantaneous responses. In consequence, it is not known how to produce mature wine in an economic framework. This study is concerned with problems that arise in a circumstance under which economic variables do not respond immediately. In particular, this study examines dynamics of an extended Solow model augmented with human capital in which physical and human capital incorporate time delays due to gestation time in physical capital and maturation time in human capital. It will be shown that the delays could destabilize an otherwise stable model and generate persistent oscillations that might be compatible with actually observed data.

Since the seminal works of Solow (1956) and Swan (1956), enormous amount of works on economic growth has carried out. There is a wide variety of topics ranging from mathematical analysis containing purely analytic works as well as empirical studies to non-technical works such as review reports of the World Bank, OECD, etc. Nevertheless, the Solow model that we call their model, following a tradition, still stays at the center of economic growth literature and many new perspectives including the current study depart from it. The Solow model itself has a quite simple structure and thus the fundamental questions of existence and stability of its steady state are easily taken care under the conventional neoclassical conditions. In spite of the simple representation of a complex economy, it can capture many real life facts. In particular, the model predicts that the living standard can be higher in a rich country in which the per capita output is higher due to the higher rate of saving and the lower rate of population whereas the living standard can be lower in a poor country in which those critical rates take reversal of those in the rich country. Mankiw, Romer and Weil (1992, MRW henceforth) empirically examine the predictions of the Solow model using a cross country example that comprises 98 countries. Some of the results that MRW obtains are favorable and others are unfavorable: the model correctly predicts the *directions* of the effects caused by changes in model's parameters such as the saving rate, the depreciation rate, the growth rates of population and the technology; however, it does not accurately give rise to the *magnitudes* of those effects, which are found to be too large. To make up for this shortcoming, MRW adopts a human capital stock as a factor in the macroeconomic production function, in addition to the physical capital stock and labor.[1] It is then empirically validated that the extended Solow model could be consistent with the international variation in the standard of living, in which about 80% of the cross-country variation in income per capita has been explained. Based on the similar model to that of MRW, Hall and Jones (1999) show that differences in the social infrastructure is crucial for the difference in per capita output between different countries. However, there is diversity of critic on MRW's contribution and model extension, see for example, Klenow

[1] Studies on human capital started in the 50s of the last century and it was revealed that investment in human capital increases the efficiency of the production fucntion.

and Rodriguez-Clare (1998) and Dinopoulos and Thompson (1999).

In comparison with the cross-country studies, there is only a smaller amount of time-series studies, mainly due to less availability of data, Jones (1995) and Greiner et al. (2005), to name only a few. It is now well known that one of the major stylized facts in advanced countries is a fluctuating positive per capita growth rate of output over time. On the other hand the Solow model predicts convergence to a steady state and no per capita growth is observed unless exogenous technical progress is present. This prediction might not be compatible with time series data. This brings us to the question of the economic conditions for which the model can be, approximately, consistent with the observable evidence. Instability property of the macro model (i.e., the knife-edge problem) addressed by Harrod (1939) and Domer (1946) which was somehow settled down by Solow (1956). After the mid 1970s, a lot of efforts have been devoted to find endogenous sources for non-convergence with applying the recently-developing chaos theory, nonlinear theory and delay theory. Initial research in this direction can be traced back to the classical seminal works in economics, a gestation delay in production by Kalecki (1935), nonlinear investment function by Kaldor (1940), delay in accelerator and nonlinear investment function by Goodwin (1951). Kalecki (1935) is the first to recognize that the capital accumulation does not often respond immediately to changes in investment but rather do so with a time delay and shows that inclusion of such time delays in investment tends to have a destabilizing influence. Since Kalecki's seminal work, it has been conjectured that a production delay could be a source of economic oscillations. Kydland and Prescot (1982) empirically confirm that a production delay could be crucial for explaining aggregate fluctuation. Recently, Zak (1999), Szydlowski and Krawiec (2004) and Guerrini et al. (2018) examine a delay Solow model for the birth of cyclic dynamics. The paper is a continuation of these studies and its main purpose is to carry out a formal stability analysis of the extended Solow model that was used to make empirical testing, however, has not been fully examined yet, especially from a dynamic view point.

The rest of the paper is organized as follows. Section 2 constructs two different versions of the extended Solow model. Section 3 examines a one-delay model. Section 4 introduces delays in physical and human capitals and investigates the two-delay effects on dynamics. Section 5 numerically validates the analytical results obtained in the previous sections. Finally concluding remarks are given in Section 6.

2 Extended Growth Model

Before proceeding the analysis, we first review the continuous-time Solow model. Only for the sake of simplicity, a Cobb-Douglas production function is adopted,

$$Y(t) = K(t)^{\alpha} \left[A(t)L(t)\right]^{1-\alpha}, \ 0 < \alpha < 1 \tag{1}$$

where t denotes time, $Y(t)$ represents output, $L(t)$ labor, $K(t)$ the physical capital stock and $A(t)$ the labor-augment technology. The physical capital accumulation is described by

$$\dot{K}(t) = sY(t) - \delta K(t) \tag{2}$$

where the dot over a variable means a time-derivative, s is the saving rate, $0 < s < 1$ and δ the depreciation rate, $\delta > 0$. Dividing the accumulation equation by effective labor $A(t)L(t)$ transforms it to a per capita form

$$\dot{k}(t) = sk(t)^{\alpha} - (n + g + \delta)k(t) \tag{3}$$

where

$$k(t) = \frac{K(t)}{A(t)L(t)},\ y(t) = \frac{Y(t)}{A(t)L(t)} = k(t)^{\alpha}$$

and the constant growth rates of labor and technology are n and g, respectively.

A positive steady state is denoted by k_S^* at which $\dot{k}(t) = 0$ for all $t \geq 0$,

$$k_S^* = \left(\frac{s}{n + g + \delta}\right)^{\frac{1}{1-\alpha}}.$$

At the steady state, the stock of physical capital and output are growing at the constant rate $n + g$,

$$\frac{\dot{K}(t)}{K(t)} = \frac{\dot{Y}(t)}{Y(t)} = n + g.$$

It is to be noticed that both growth rates are exogenously given and thus the growth of per capita output occurs only due to exogenous technology change.

In the following, we further summarize two versions of the extended Solow model augmented with human capital.

2.1 Jones Version

Jones (1998) replaces labor with the human capital in the production function,

$$Y(t) = K(t)^{\alpha} \left[A(t)H(t)\right]^{1-\alpha}$$

showing H, the stock of the human capital, is related with labor L according to

$$H(t) = e^{\phi(E)}L(t)$$

showing that H is a result of labor trained with E years of schooling (education) and $\phi(E)$ with $\phi'(E) > 0$ and $\phi(0) = 0$ reflects the efficiency of a unit labor with E years of education to one with no education. The Jones version is identical with the Solow model when $E = 0$. Dividing the production function by $A(t)H(t)$ gives

$$\tilde{y}(t) = \tilde{k}(t)^{\alpha}$$

where

$$\tilde{y} = \frac{y}{Ae^{\phi(E)}} \text{ and } \tilde{k} = \frac{k}{Ae^{\phi(E)}}.$$

The accumulation of the physical capital per capita is, dropping tilde from $\tilde{y}$ and $\tilde{k}$,

$$\dot{k}(t) = sy(t) - (n + g + \delta)k(t). \tag{4}$$

This equation (4) is essentially the same as the accumulation equation (3) of the Solow model, implying that replacing labor with human capital does not affect the basic properties of the Solow model. The larger saving rate leads to a larger per capita output while the larger rate of population decreases the per capita output, as in the Solow model,

$$\frac{\partial y}{\partial s} > 0 \text{ and } \frac{\partial y}{\partial n} < 0.$$

2.2 MRW version

MRW assumes an extended Cobb-Douglas production function to have three factors,

$$Y(t) = K(t)^{\alpha} H(t)^{\beta} \left[A(t)L(t)\right]^{1-\alpha-\beta}$$

where $1 - \alpha - \beta > 0,\ \alpha > 0$ and $\beta > 0$. H is the stock of human capital and defined differently from Jones (1998). Physical capital and human capital are formed by saving a s_k-fraction and s_h-fraction of output with $s_k > 0$, $s_h > 0$ and $s_k + s_h < 1$. The accumulation of these per capita capital stocks is determined by

$$\begin{aligned} \dot{k}(t) &= s_k k(t)^{\alpha} h(t)^{\beta} - (n + g + \delta)k(t) \\ \dot{h}(t) &= s_h k(t)^{\alpha} h(t)^{\beta} - (n + g + \delta)h(t) \end{aligned} \tag{5}$$

where $k(t)$ is already defined and $h(t)$ is the stock of human capital per capita defined by

$$h(t) = \frac{H(t)}{A(t)L(t)}.$$

A steady state is defined by

$$\begin{aligned} k^* &= \left(\frac{s_k^{1-\beta} s_h^{\beta}}{n + g + \delta}\right)^{\frac{1}{1-\alpha-\beta}}, \\ h^* &= \left(\frac{s_k^{\alpha} s_h^{1-\alpha}}{n + g + \delta}\right)^{\frac{1}{1-\alpha-\beta}}. \end{aligned} \tag{6}$$

Nonnegative values of k^* and h^* lead the following conditions at the steady state at which $\dot{k}(t) = \dot{h}(t) = 0$,

$$\begin{aligned} s_k \left(k^*\right)^{\alpha-1} \left(h^*\right)^{\beta} &= c, \\ s_h \left(k^*\right)^{\alpha} \left(h^*\right)^{\beta-1} &= c \end{aligned} \tag{7}$$

with $n+g+\delta=c$. As shown shortly after, the dynamic system (5) converges to the steady state under the assumption of diminishing returns to scale (i.e., $\alpha+\beta<1$):

Theorem 1 *The positive stationary point* (h^*, k^*) *of extended Solow model (5) is locally asymptotically stable.*

To assert stability graphically, Figure 1 illustrates a phase diagram in which the red curve describes the $\dot{k}(t)=0$ locus and the blue curve the $\dot{h}(t)=0$ locus.[2] It can be seen that as indicated by arrows, all trajectories approach the stationary point that is the positive intersection of the red and blue curves. The physical capital, human capital and output grow at the same rate of $n+g$, as in the Solow model,

$$\frac{\dot{K}(t)}{K(t)}=\frac{\dot{H}(t)}{H(t)}=\frac{\dot{Y}(t)}{Y(t)}=n+g$$

while the per capita variables are on the balanced growth path and grow at the exogenously given rate of the technology change,

$$\frac{\dot{k}(t)}{k(t)}=\frac{\dot{h}(t)}{h(t)}=\frac{\dot{y}(t)}{y(t)}=g.$$

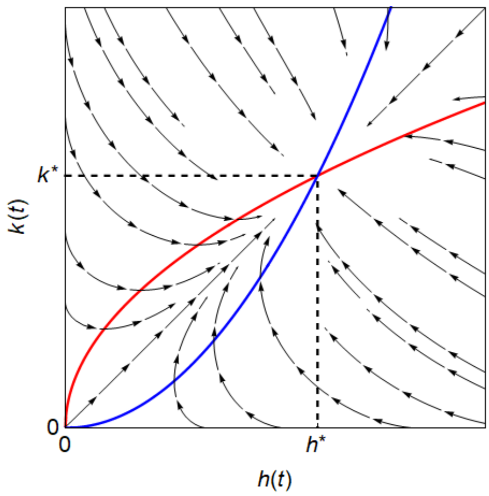

Figure 1. Phase diagram of no-delay model (5)

3 One Delay Model

The Jones version, which is essentially the same as the Solow model, could be a prototype model embodying the human capital. Its dynamics has two phases. In

[2] The parameter values are specified only for the sake simplicity as follows,

$$s_k=s_h=3/10,\ c=1/10 \text{ and } \alpha=\beta=1/3.$$

Any other values are possible and generate essentially the same phase diagram.

the first phase, the economy starting at any initial state sooner or later converges to the steady state. On a transition path to the steady state, per capita growth is positive and becomes zero when it arrives at the steady state. In the second phase the long-run dynamics is conducted by the population growth and the technological development. We focus on the evolution of the economy in the first phase. To this end, we assume the following to get rid of the exogenous shocks.

Assumption $n = g = 0$.

Further, if we consider the Kaleckian gestation delay τ in the production process, the per capita capital stock at time t in continuous time is expressed by

$$k(t) = \int_{-\infty}^{t-\tau} i(T)e^{-\delta[(t-\tau)-T]}dT$$

where $i(T)$ is investment at time T,

$$i(T) = sk(T)^a.$$

Differentiating this equation with respect to t yields the delay equation of capital accumulation,

$$\dot{k}(t) = sk(t-\tau)^a - \delta k(t). \tag{8}$$

If the capital starts depreciation after it is installed, then equation (8) should be

$$\dot{k}(t) = sk(t-\tau)^a - \delta k(t-\tau). \tag{9}$$

Guerrini et al. (2019) show that a steady state of equation (8) is locally asymptotically stable for any value of τ and also that there is a critical value τ_0 such that the steady state of equation (9) is locally asymptotically stable for $\tau < \tau_0$ and unstable for $\tau > \tau_0$. Science the Jones version of the extended Solow model has essentially the same dynamic structure as that of the Solow model, if it has a delay only in the production process, then the delay is harmless and if there is also a delay in depreciation, then the delay version can be unstable and might generate cyclic oscillations of the per capita variables.

We now turn attention to delay version of MRS stock accumulation system of physical and human capitals

$$\begin{aligned} \dot{k}(t) &= s_k k(t-\tau_k)^\alpha h(t-\tau_h)^\beta - \delta k(t-\tau_k) \\ \dot{h}(t) &= s_h k(t-\tau_k)^\alpha h(t-\tau_h)^\beta - \delta h(t-\tau_h) \end{aligned} \tag{10}$$

with $\tau_k \geq 0$ and $\tau_h \geq 0$. Linearizing each equation of (10) gives

$$\dot{k}(t) = \left[\alpha s_k (k^*)^{\alpha-1} (h^*)^\beta - \delta\right] k(t-\tau_k) + \beta s_k (k^*)^\alpha (h^*)^{\beta-1} h(t-\tau_h),$$

$$\dot{h}(t) = \alpha s_h (k^*)^{\alpha-1} (h^*)^\beta k(t-\tau_k) + \left[\beta s_h (k^*)^\alpha (h^*)^{\beta-1} - \delta\right] h(t-\tau_h).$$

Using the relations in (7) yields the linearized delay system,

$$\dot{k}(t) = \delta(\alpha - 1)k(t - \tau_k) + \beta\delta\frac{s_k}{s_h}h(t - \tau_k),$$
$$\dot{h}(t) = \alpha\delta\frac{s_h}{s_k}k(t - \tau_h) + \delta(\beta - 1)h(t - \tau_h). \tag{11}$$

The corresponding characteristic equation is

$$\left\{\lambda - \delta(\alpha - 1)e^{-\lambda\tau_k}\right\}\left\{\lambda - \delta(\beta - 1)e^{-\lambda\tau_h}\right\} - \alpha\beta\delta^2 e^{-\lambda(\tau_k+\tau_h)} = 0$$

or

$$P_0(\lambda) + P_1(\lambda)e^{-\lambda\tau_k} + P_2(\lambda)e^{-\lambda\tau_h} + P_3(\lambda)e^{-\lambda(\tau_k+\tau_h)} = 0 \tag{12}$$

where

$$P_0(\lambda) = \lambda^2,$$
$$P_1(\lambda) = \delta(1 - \alpha)\lambda,$$
$$P_2(\lambda) = \delta(1 - \beta)\lambda,$$
$$P_3(\lambda) = \delta^2\left(1 - \alpha - \beta\right).$$

As a benchmark, we start with the no-delay case in which $\tau_k = \tau_h = 0$. The characteristic equation (12) is now written as

$$\lambda^2 + \delta\left[(1 - \alpha) + (1 - \beta)\right]\lambda + \delta^2\left(1 - \alpha - \beta\right) = 0. \tag{13}$$

Since the linear coefficient and the constant term are both positive, the roots are either real negative or complex with negative real parts implying asymptotical stability. This result without Assumption (that is, δ should be replaced with c) proves Theorem 1 that shows local stability of the stationary state in the no-delay model, (5).

We next consider a one-delay case of $\tau_k = \tau_h = \tau$, a first approximation of the circumstance in which a difference between gestation time and the maturation time is small. The corresponding characteristic equation is obtained from (12) with appropriate replacement,

$$\lambda^2 + \delta(2 - \alpha - \beta)\lambda e^{-\lambda\tau} + \delta^2(1 - \alpha - \beta)e^{-2\lambda\tau} = 0$$

or multiplying both sides by $e^{\lambda\tau}$ transforms it to

$$\lambda^2 e^{\lambda\tau} + \delta(2 - \alpha - \beta)\lambda + \delta^2(1 - \alpha - \beta)e^{-\lambda\tau} = 0. \tag{14}$$

Suppose that $\lambda = i\omega$ with $\omega > 0$ is a root of (14) for some τ. Separating the real and imaginary parts presents two equations,

$$\left[\delta^2\left(1 - \alpha - \beta\right) - \omega^2\right]\cos\omega\tau = 0,$$
$$-\left[\delta^2\left(1 - \alpha - \beta\right) + \omega^2\right]\sin\omega\tau + \delta(2 - \alpha - \beta)\omega = 0. \tag{15}$$

If we assume $\omega^2 = \delta^2 (1-\alpha-\beta)$ in the first equation of (15), then the second equation leads to

$$\sin \omega\tau = \frac{2-\alpha-\beta}{2\sqrt{1-\alpha-\beta}} > 1$$

where the inequality is due to

$$[1+(1-\alpha-\beta)]^2 - 4(1-\alpha-\beta) = (\alpha+\beta)^2 > 0.$$

Hence we have the following from the first equation,

$$\cos\omega\tau = 0 \text{ and } \sin\omega\tau = \pm 1.$$

If $\sin\omega\tau = -1$, then the second equation becomes

$$\omega^2 + \delta(2-\alpha-\beta)\omega + \delta^2 (1-\alpha-\beta) = 0$$

that is identical with (13), implying that both roots are either real negative or complex with negative real parts. No stability switch occurs. If $\sin\omega\tau = +1$, then the second equation,

$$\omega^2 - \delta(2-\alpha-\beta)\omega + \delta^2 (1-\alpha-\beta) = 0$$

yields two positive roots,

$$\omega_\pm = \frac{1}{2}\left\{\delta(2-\alpha-\beta) \pm \sqrt{\delta^2(2-\alpha-\beta)^2 - 4\delta^2 (1-\alpha-\beta)}\right\}$$

that is further reduced to

$$\omega_- = \omega(1-\alpha-\beta) \text{ and } \omega_+ = \delta.$$

Hence the critical values of the delay are

$$\tau_{+,n} = \frac{1}{\omega_+}\left(\frac{\pi}{2} + 2n\pi\right) \text{ and } \tau_{-,n} = \frac{1}{\omega_-}\left(\frac{\pi}{2} + 2n\pi\right) \text{ for } n = 0, 1, 2, \ldots .$$

We need to determine the sign of the derivative of $\mathrm{Re}\,[\lambda(\tau)]$ in order to verify the direction of stability switching. Differentiating (14) with respect to τ at the point where $\lambda(\tau)$ is purely imaginary, we have

$$\left\{2\lambda e^{\lambda\tau} + \delta(2-\alpha-\beta) + \tau\left[\lambda^2 e^{\lambda\tau} - \delta^2(1-\alpha-\beta)e^{-\lambda\tau}\right]\right\}\frac{d\lambda}{d\tau}$$

$$= -\lambda\left[\lambda^2 e^{\lambda\tau} - \delta^2(1-\alpha-\beta)e^{-\lambda\tau}\right].$$

For convenience, we study $(d\lambda/d\tau)^{-1}$, instead of $d\lambda/d\tau$,

$$\left(\frac{d\lambda}{d\tau_k}\right)^{-1} = \frac{2\lambda e^{\lambda\tau} + \delta(2-\alpha-\beta)}{-\lambda\left[\lambda^2 e^{\lambda\tau} - \delta^2(1-\alpha-\beta)e^{-\lambda\tau}\right]} - \frac{\tau}{\lambda}$$

$$= -\frac{1}{\lambda^2} - \frac{\tau}{\lambda}$$

where (14) is used from the first step to the second step. Therefore inserting $\lambda = i\omega_+$ with $\omega = \omega_+$ or $\omega = \omega_-$ and taking the real part gives

$$\mathrm{Re}\left[\left(\frac{d\lambda}{d\tau}\right)^{-1}_{\lambda=i\omega}\right] = \mathrm{Re}\left[\frac{1}{\omega^2} - \frac{\tau}{i\omega}\right] = \frac{1}{\omega^2} > 0.$$

The last inequality implies that the crossing of the imaginary axis is from left to right at all critical values. Therefore stability is lost at the smallest critical value $\tau_{+,0}$ and stability cannot be regained later.

Theorem 2 *The stationary state of the delay MRS model (10) with $\tau_x = \tau_y = \tau$ is locally asymptotically stable for $\tau < \tau_{+,0}$ and unstable for $\tau > \tau_{+,0}$. Furthermore, it undergoes a Hopf bifurcation at $\tau > \tau_{+,0}$ where $\tau_{+,0}$ is the smallest critical value and defined as*

$$\tau_{+,0} = \frac{\pi}{2\omega_+}.$$

4 Two Delay Model

We now suppose that $\tau_k > 0$ and $\tau_h > 0$ and find all pure complex roots of the characteristic equation of (12).[3] We can also assume that $\lambda = i\omega$ with $\omega > 0$. Substituting this solution into (12) presents the following form of the characteristic equation,

$$P_0(i\omega) + P_1(i\omega)e^{-i\omega\tau_k} + P_2(i\omega)e^{-i\omega\tau_h} + P_3(i\omega)e^{-i\omega(\tau_k+\tau_h)} = 0 \qquad (16)$$

where

$$P_0(i\omega) = -\omega^2,$$

$$P_1(i\omega) = i\delta(1-\alpha)\omega,$$

$$P_2(i\omega) = i\delta(1-\beta)\omega,$$

$$P_3(i\omega) = \delta^2\left(1-\alpha-\beta\right).$$

Applying the method developed by Matsumoto and Szidarovszky (2018) based on Lin and Wang (2012), we can derive the set of points (τ_k, τ_h) for which the delay dynamic system (10) might lose stability. Equation (16) can be written as

$$P_0(i\omega) + P_1(i\omega)e^{-i\omega\tau_k} + \left(P_2(i\omega) + P_3(i\omega)e^{-i\omega\tau_k}\right)e^{-i\omega\tau_h} = 0. \qquad (17)$$

Since $\left|e^{-\lambda\tau_h}\right| = 1$, equation (17) has solution if and only if

$$\left|P_0(i\omega) + P_1(i\omega)e^{-i\omega\tau_k}\right| = \left|P_2(i\omega) + P_3(i\omega)e^{-i\omega\tau_k}\right|$$

[3] It is possible to introduce two different delays into the Jones model. See Guerrini et al. (2018).

or equivalently,

$$\begin{aligned} & \left(P_0(i\omega) + P_1(i\omega)e^{-i\omega\tau_k}\right)\left(\bar{P}_0(i\omega) + \bar{P}_1(i\omega)e^{i\omega\tau_k}\right) \\ = & \left(P_2(i\omega) + P_3(i\omega)e^{-i\omega\tau_k}\right)\left(\bar{P}_2(i\omega) + \bar{P}_3(i\omega)e^{i\omega\tau_k}\right) \end{aligned}$$

where over-bar indicates complex conjugate. After some calculations, the last equation can be rewritten as

$$|P_0|^2 + |P_1|^2 - |P_2|^2 - |P_3|^2 = 2A_k(\omega)\cos\omega\tau_k - 2B_k(\omega)\sin\omega\tau_k \tag{18}$$

where the argument of P_i is omitted for the sake of notational simplicity and

$$A_k(\omega) = \mathrm{Re}\left(P_2\bar{P}_3 - P_0\bar{P}_1\right) \text{ and } B_k(\omega) = \mathrm{Im}\left(P_2\bar{P}_3 - P_0\bar{P}_1\right).$$

Using $P_i(i\omega)$ for $i = 0, 1, 2, 3$, we can obtain

$$P_2\bar{P}_3 - P_0\bar{P}_1 = ic\omega\left[\delta^2(1-\beta)(1-\alpha-\beta) - \omega^2(1-\alpha)\right].$$

Hence

$$A_k(\omega) = 0$$

and

$$B_k(\omega) = \delta\omega\left[\delta^2(1-\beta)(1-\alpha-\beta) - \omega^2(1-\alpha)\right].$$

The sign of $B_k(\omega)$ is indeterminate. Denoting the left hand side of equation (18) by $f(\omega)$, we confirm solutions of (18), that is, $f(\omega) = -2B_k(\omega)\sin\omega\tau_k$. We first examine the case of $B_k(\omega) = 0$ and then proceed to the case of $B_k(\omega) \neq 0$.

4.1 Case I: $B_k(\omega) = 0$

Let ω_k be the positive solution of $B_k(\omega) = 0$,

$$\omega_k = \delta\sqrt{\frac{(1-\beta)(1-\alpha-\beta)}{1-\alpha}} > 0.$$

Substituting $P_i(i\omega)$ for $i = 0, 1, 2, 3$ into $f(\omega)$ gives

$$f(\omega) = \omega^4 + \delta^2(\beta-\alpha)(2-\alpha-\beta)\omega^2 - \delta^4(1-\alpha-\beta)^2.$$

Solving $f(\omega) = 0$ for ω^2 presents a positive solution,

$$\omega_+^2 = \frac{-\delta^2(\beta-\alpha)(2-\alpha-\beta) + \sqrt{\delta^4(\beta-\alpha)^2(2-\alpha-\beta)^2 + 4\delta^4(1-\alpha-\beta)^2}}{2} > 0.$$

If $\alpha = \beta$, then the critical value and the positive solution become identical,

$$\omega_k^2 = \omega_+^2 = \delta^2(1-2\alpha) > 0$$

and if $\alpha \neq \beta$, then $\omega_k^2 \neq \omega_+^2$ since it is easy to see that $f(\omega_k) \neq 0$. Thus there is no solution for τ_k since equation (18) is contradicted. On the other hand, if

$\alpha = \beta$, then $f_k(\omega) = 0$ for $\omega = \omega_k$ and the corresponding values of τ_h can be obtained from equation (17) as

$$e^{-i\omega\tau_h} = -\frac{P_0(i\omega) + P_1(i\omega)e^{-i\omega\tau_k}}{P_2(i\omega) + P_3(i\omega)e^{-i\omega\tau_k}} \tag{19}$$

where the absolute value of the right hand side is unity for all values of τ_k. Therefore there are infinitely many solutions of τ_h because of trigonometric functions. A locus of τ_k and τ_h satisfying (19) is called a *crossing curve* on which roots of (17) cross the imaginary axis when τ_i changes and τ_j is fixed $(i, j = k, h,\ i \neq j,)$. Since the zero solution of (11) is locally asymptotically stable in case of no delays and stability with positive delays could depend on their lengths, there might be a curve on which the stability of the steady state changes.

An explicit form of τ_h satisfying equation (19) is derived as follows. Due to the Euler's formula, (19) can be rewritten as

$$\cos\omega\tau_h - i\sin\omega\tau_h = \frac{\omega^2 - \delta\omega(1-\alpha)\sin\omega\tau_k - i\delta\omega(1-\alpha)\cos\omega\tau_k}{\delta^2(1-\alpha-\beta)\cos\omega\tau_k + i\left[\delta\omega(1-\beta) - \delta^2(1-\alpha-\beta)\sin\omega\tau_k\right]}. \tag{20}$$

The right hand side is next developed. Multiplying the denominator and the numerator of (20) by the conjugate of the denominator, the denominator, after arranging the terms, becomes

$$D = \delta^2\left[\delta^2(1-\alpha-\beta)^2 + \omega^2(1-\beta)^2 - 2\delta\omega(1-\beta)(1-\alpha-\beta)\sin\omega\tau_k\right].$$

The new numerator can be denoted by $M + iN$ where the real part is

$$M = -(\delta\omega)^2\alpha\beta\cos\omega\tau_k$$

and the imaginary part is

$$N = -\delta\omega\left\{\delta^2(1-\alpha)(1-\alpha-\beta) + \omega^2(1-\beta) - \delta\omega\left[2(1-\alpha-\beta) + \alpha\beta\right]\sin\omega\tau_k\right\}.$$

Comparing the left hand side of (20) with $M/D + iN/D$ presents

$$\cos\omega\tau_h = \frac{M}{D} \text{ and } \sin\omega\tau_h = -\frac{N}{D}. \tag{21}$$

The graphs of M/D and $-N/D$ are illustrated for $\tau_k \in \left[0, 20\sqrt{3}\pi/\omega\right]$ with the benchmark parameter values of $\alpha = 1/3,\ \beta = 1/3$ and $\delta = 1/10$ in Figure 2. The red M/D curve intersects the horizontal axis twice at which $\cos\omega\tau_k = 0$, implying that $\omega\tau_k = \pi/2$ at point B and $\omega\tau_k = 3\pi/2$ at point D,

$$\tau_k^B = \frac{\pi}{2\omega_k} \simeq 24.72 \text{ and } \tau_k^D = \frac{3\pi}{2\omega_k} \simeq 81.62.$$

It is also seen that the blue $-N/D$ curve intersects the horizontal axis twice at which $N = 0$ or

$$\begin{aligned}\sin\omega\tau_k &= \frac{\delta^2(1-\alpha)(1-\alpha-\beta) + \omega_k^2(1-\beta)}{\delta\omega_k\left[2(1-\alpha-\beta) + \alpha\beta\right]} \\ &= \frac{2(1-\alpha)\sqrt{1-2\alpha}}{(\alpha-2)^2 - 2} < 1 \text{ for } 0 < \alpha < \frac{1}{2}.\end{aligned}$$

Since $\sin \omega\tau_k$ takes the maximum value at $\omega\tau_k = \pi/2$, $\sin \omega\tau_k^A = 4\sqrt{3}/7$ and $\cos \omega\tau_k^A > 0$ at point A and $\sin \omega\tau_k^B = 4\sqrt{3}/7$ and $\cos \omega\tau_k^B < 0$ at point B, implying that

$$\tau_k^A = \frac{1}{\omega_k} \sin^{-1}\left(\frac{4\sqrt{3}}{7}\right) \simeq 24.72 \text{ and } \tau_k^C = \frac{1}{\omega_k}\left[\pi - \sin^{-1}\left(\frac{4\sqrt{3}}{7}\right)\right] \simeq 29.69.$$

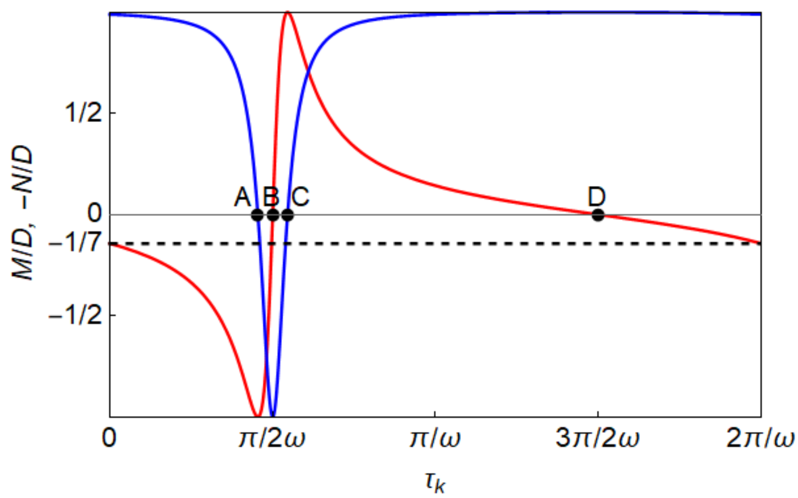

Figure 2. Graphs of M/D (red) and $-N/D$ (blue)

The interval $[0, 2\pi/\omega_k]$ is divided into five subintervals by those points. It is observed that $\cos \omega\tau_h < 0$ and $\sin \omega\tau_h > 0$ for $\tau_k \in (0, \tau_k^A)$. Hence solving $\cos \omega_k\tau_h = M/D$ and $\sin \omega_k\tau_h = -N/D$ for τ_h yields

$$\tau_h^c(\tau_k) = \frac{1}{\omega_k} \cos^{-1}\left(\frac{M}{D}\right) \text{ and } \tau_h^s(\tau_k) = \frac{1}{\omega_k}\left[\pi - \sin^{-1}\left(-\frac{N}{D}\right)\right]. \tag{22}$$

where the superscripts c and s stand for cos and sin, respectively. In the same way, $\cos \omega_k\tau_h < 0$ and $\sin \omega_k\tau_h < 0$ for $\tau_h \in (\tau_k^A, \tau_k^B)$ that present

$$\tau_h^c(\tau_k) = \frac{1}{\omega_k}\left[2\pi - \cos^{-1}\left(\frac{M}{D}\right)\right] \text{ and } \tau_h^s(\tau_k) = \frac{1}{\omega_k}\left[\pi - \sin^{-1}\left(-\frac{N}{D}\right)\right]. \tag{23}$$

For $\tau_k \in (\tau_k^B, \tau_k^C)$, $\cos \omega_k\tau_k > 0$ and $\sin \omega_k\tau_k < 0$ gives

$$\tau_h^c(\tau_k) = \frac{1}{\omega_k}\left[2\pi - \cos^{-1}\left(\frac{M}{D}\right)\right] \text{ and } \tau_h^s(\tau_k) = \frac{1}{\omega_k}\left[2\pi + \sin^{-1}\left(-\frac{N}{D}\right)\right]. \tag{24}$$

For $\tau_k \in (\tau_k^C, \tau_k^D)$, $\cos \omega_h\tau_k > 0$ and $\sin \omega_h\tau_k > 0$ generating

$$\tau_h^c(\tau_k) = \frac{1}{\omega_k} \cos^{-1}\left(\frac{M}{D}\right) \text{ and } \tau_h^s(\tau_k) = \frac{1}{\omega_k} \sin^{-1}\left(-\frac{N}{D}\right). \tag{25}$$

Finally, we have $\cos\omega_h\tau_k < 0$ and $\sin\omega_h\tau_k > 0$ for $\tau_k \in (\tau_k^D, 2\pi/\omega_k)$ in which case the signs of the trigonometric functions are the same as in the first case. Hence, from (22)

$$\tau_h^c(\tau_k) = \frac{1}{\omega_k}\cos^{-1}\left(\frac{M}{D}\right) \text{ and } \tau_h^s(\tau_k) = \frac{1}{\omega_k}\left[\pi - \sin^{-1}\left(-\frac{N}{D}\right)\right]. \tag{26}$$

Since $\tau_h^s(\tau_k) = \tau_h^c(\tau_k)$ holds for any $\tau_k \in [0, 2\pi/\omega]$, the solution can be denoted by $\tau_h(\tau_k)$.

The locus of $(\tau_k, \tau_h(\tau_k))$ for $\tau_k \in [0, 2\pi/\omega]$ constructs the crossing curve in Case I that is illustrated by two black-red curves in Figure 3. More precisely, the upper convex-shaped curve consists of three segments, each of which is described by the black segment (22), the red segment, (23) and the black segment, (24) whereas the lower concave-shaped curve is described by the red segment (25) and the black segment, (26). The results obtained are summarized as follows:

Theorem 3 *If $B_k(\omega) = 0$ and $\alpha = \beta$, then the crossing curve is described by the locus of $(\tau_k, \tau_h(\tau_k))$ where*

$$\tau_h(\tau_k) = \frac{1}{\omega_k}\cos^{-1}\left(\frac{M}{D}\right) \quad \textit{for } \tau_k \in (0, \tau_k^A) \cup (\tau_k^C, \tau_k^D) \cup (\tau_k^D, 2\pi/\omega_k)$$

and

$$\tau_h(\tau_k) = \frac{1}{\omega_k}\left[2\pi - \cos^{-1}\left(\frac{M}{D}\right)\right] \quad \textit{for for } \tau_k \in (\tau_k^A, \tau_k^B) \cup (\tau_k^B, \tau_k^C).$$

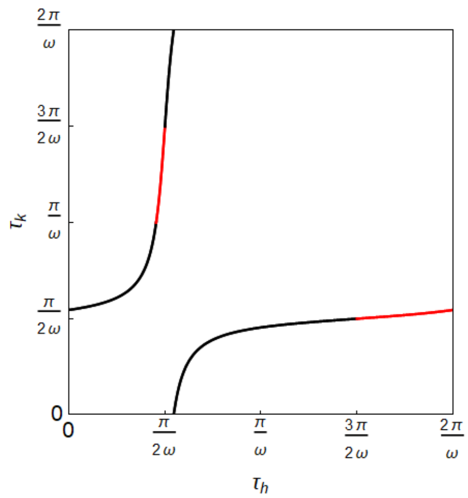

Figure 3. Crossing curve with $B_k(\omega) = 0$ and $\alpha = \beta$

4.2 Case II: $|B_k(\omega)|^2 > 0$

We have already shown that $A_k(\omega) = 0$ for any $\omega \geq 0$ and $B_k(\omega) \neq 0$ for $\omega \neq \omega_k$. Then there exists $\varphi_k(\omega)$ such that

$$\varphi_k(\omega) = \arg\left[P_2\bar{P}_3 - P_0\bar{P}_1\right] = \begin{cases} \dfrac{\pi}{2} \text{ if } B_k(\omega) > 0 \text{ or } \omega < \omega_k, \\ \\ \dfrac{3\pi}{2} \text{ if } B_k(\omega) < 0 \text{ or } \omega > \omega_k, \end{cases}$$

implying that

$$\sin\left[\varphi_k(\omega)\right] = \frac{B_k(\omega)}{\sqrt{B_k(\omega)^2}} = 1 \text{ and } \cos\left[\varphi_k(\omega)\right] = \frac{A_k(\omega)}{\sqrt{B_k(\omega)^2}} = 0.$$

Using these relations and the addition theorem, equation (18) can be reduced to

$$|P_0|^2 + |P_1|^2 - |P_2|^2 - |P_3|^2 = 2\sqrt{B_k(\omega)^2}\cos\left[\varphi_k(\omega) + \omega\tau_k\right] \tag{27}$$

that can be rewritten as

$$\frac{|P_0|^2 + |P_1|^2 - |P_2|^2 - |P_3|^2}{2\sqrt{B_k(\omega)^2}} = \cos\left[\varphi_k(\omega) + \omega\tau_k\right] \leq 1.$$

Hence a sufficient and necessary condition for the existence of $\tau_k \geq 0$ satisfying the above equation is

$$\left| |P_0|^2 + |P_1|^2 - |P_2|^2 - |P_3|^2 \right| \leq 2\sqrt{B_k(\omega)^2}$$

or

$$F(\omega) = \left[|P_0|^2 + |P_1|^2 - |P_2|^2 - |P_3|^2\right]^2 - 4B_k(\omega)^2 \leq 0.$$

With the notation of $x = \omega^2$, the right hand side of $F(\omega)$ is reduced to the following form,

$$F(x) = x^4 + a_3x^3 + a_2x^2 + a_1x + a_0 \tag{28}$$

where the coefficients are defined as

$$a_3 = -2\delta^2\left[(1-\alpha)^2 + (1-\beta)^2\right],$$

$$a_2 = \delta^4\left\{\left[(1-\alpha)^2 - (1-\beta)^2\right]^2 - 2(1-\alpha-\beta)\left[4(1-\alpha)(1-\beta) + (1-\alpha-\beta)\right]\right\},$$

$$a_1 = -2\delta^6(1-\alpha-\beta)^2\left[(1-\alpha)^2 + (1-\beta)^2\right],$$

$$a_0 = \delta^8(1-\alpha-\beta)^4.$$

The factored form of (28) becomes

$$F(x) = \left(x - \delta^2\right)\left(x - \delta^2(1-\alpha-\beta)^2\right)\eta(x) \tag{29}$$

where

$$\eta(x) = x^2 - \delta^2 \left[(\alpha-\beta)^2 + 2(1-\alpha-\beta) \right] x + \delta^4 (1-\alpha-\beta)^2 .$$

Solving $F(x) = 0$ yields four real solutions,

$$x_1 = \delta^2 > 0,$$

$$x_2 = \delta^2 (1-\alpha-\beta)^2 > 0,$$

$$x_3 = \frac{\delta^2}{2} \left[(\alpha-\beta)^2 + 2(1-\alpha-\beta) - (\alpha-\beta) \sqrt{(\alpha-\beta)^2 + 2(1-\alpha-\beta)} \right],$$

$$x_4 = \frac{\delta^2}{2} \left[(\alpha-\beta)^2 + 2(1-\alpha-\beta) + (\alpha-\beta) \sqrt{(\alpha-\beta)^2 + 2(1-\alpha-\beta)} \right].$$

It is to be notice that $\eta(0) > 0$ and $\eta'(0) < 0$ implying $x_3 < x_4$ with $\eta'(x_3) < 0$ and $\eta'(x_4) > 0$ if $\alpha > \beta$ and the inequalities are reversed if $\alpha < \beta$. In the following, we suppose $\alpha > \beta$ only for the sake of convenience. It is clear that $x_1 > x_2 > 0$ as $1 > \alpha + \beta,\ \alpha > 0$ and $\beta > 0$ are already assumed. Further substituting x_1 and x_2 into $\eta(x)$ gives

$$\eta(x_1) = 4\delta^2\alpha\beta > 0 \text{ and } \eta(x_2) = 4\delta^2\alpha\beta (1-\alpha-\beta)^2 > 0.$$

The derivative of $\eta(x)$ evaluated at $x = x_1$ is

$$\eta'(x_1) = \delta^2 \left[2(\alpha+\beta) - (\alpha-\beta)^2 \right] > 0$$

where the inequality is due to

$$2(\alpha+\beta) - (\alpha-\beta)^2 > 2(\alpha+\beta) - (\alpha+\beta)^2 = (\alpha+\beta)(2-\alpha-\beta) > 0.$$

The derivative of $\eta(x)$ evaluated at $x = x_2$ is

$$\begin{aligned} \eta'(x_2) &= 2\delta^2(1-\alpha-\beta)^2 - \delta^2 \left[(\alpha-\beta)^2 + 2(1-\alpha-\beta) \right] \\ &= -\delta^2 \left[2(1-\alpha-\beta)(\alpha+\beta) + (\alpha-\beta)^2 \right] < 0. \end{aligned}$$

Then

$$\eta(x_1) > 0 \text{ and } \eta'(x_1) > 0 \text{ implying that } x_4 < x_1$$

and

$$\eta(x_2) > 0 \text{ and } \eta'(x_2) < 0 \text{ implying that } x_2 < x_3.$$

Therefore we have

$$0 < x_2 < x_3 < x_4 < x_1.$$

Let ω_i be a positive solution of $x_i = \omega^2$, then

$$0 < \omega_2 < \omega_3 < \omega_4 < \omega_1.$$

The interval union $[\omega_2, \omega_3] \cup [\omega_4, \omega_1]$ is denoted by Ω in which $F(\omega) \leq 0$.

Let us define $\psi_k(\omega)$ by

$$|P_0|^2 + |P_1|^2 - |P_2|^2 - |P_3|^2 = 2\sqrt{B_k(\omega)^2} \cos[\psi_k(\omega)] \tag{30}$$

or

$$\psi_k(\omega) = \cos^{-1}\left[\frac{|P_0|^2 + |P_1|^2 - |P_2|^2 - |P_3|^2}{2\sqrt{B_k(\omega)^2}}\right].$$

Comparing the right hand side of (27) with that of (30) presents

$$\tau_{k,m}^{\pm}(\omega) = \frac{1}{\omega}\left[\pm\psi_k(\omega) - \varphi_k(\omega) + 2m\pi\right]. \tag{31}$$

Returning to (16), we can see that it can be alternatively written as

$$\left(P_0 + P_2 e^{-i\omega\tau_h}\right) + \left(P_1 + P_3 e^{-i\omega\tau_h}\right) e^{-i\omega\tau_k} = 0. \tag{32}$$

The similarity of (32) to (17) is clear. Hence, in the similar way to deriving $\tau_{k,m}^{\pm}(\omega)$, we can define the critical values of τ_h as

$$\tau_{h,n}^{\pm}(\omega) = \frac{1}{\omega}\left[\pm\psi_h(\omega) - \varphi_h(\omega) + 2n\pi\right] \tag{33}$$

where

$$\begin{aligned} A_h(\omega) &= \mathrm{Re}\left[P_1\bar{P}_3 - P_0\bar{P}_2\right] = 0, \\ B_h(\omega) &= \mathrm{Im}\left[P_1\bar{P}_3 - P_0\bar{P}_2\right] = \delta\omega\left[\delta^2(1-\alpha)(1-\alpha-\beta) - \omega^2(1-\beta)\right], \end{aligned}$$

$$\psi_h(\omega) = \cos^{-1}\left[\frac{|P_0|^2 - |P_1|^2 + |P_2|^2 - |P_3|^2}{2\sqrt{B_h(\omega)^2}}\right]$$

and

$$\varphi_h(\omega) = \arg\left[P_1\bar{P}_3 - P_0\bar{P}_2\right] = \begin{cases} \dfrac{\pi}{2} & \text{if } B_h(\omega) > 0 \text{ or } \omega < \omega_h, \\[2ex] \dfrac{3\pi}{2} & \text{if } B_h(\omega) < 0 \text{ or } \omega > \omega_h \end{cases}$$

with ω_h being the positive solution of $B_h(\omega) = 0$.

In case of $B_h(\omega) = 0$, we solve (32) to have

$$e^{-i\omega\tau_k} = \frac{P_0 + P_2 e^{-i\omega\tau_h}}{P_1 + P_3 e^{-i\omega\tau_h}}. \tag{34}$$

Two remarks should be addressed. First, as in the same way as to derive $\tau_h(\tau_k)$ from equation (19), we can obtain $\tau_k(\tau_h)$ and the crossing curve $(\tau_k(\tau_h), \tau_h)$ from equation (34). Secondly, noticing that (19) and (34) are different equations derived from the same equation (17), we can see that the crossing curve

$(\tau_k(\tau_h), \tau_h)$ is identical with the crossing curve $(\tau_h(\tau_k), \tau_k)$. In case of $B_h(\omega) \neq 0$, we can define critical values of τ_h. To define $\psi_h(\omega)$, we need a condition similar to $F(\omega) \leq 0$, that is,

$$G(\omega) = \left[|P_0|^2 - |P_1|^2 + |P_2|^2 - |P_3|^2 \right]^2 - 4B_h(\omega)^2 \leq 0.$$

Since it can be shown that $F(\omega) = G(\omega)$, solutions of $F(\omega) = 0$ and $G(\omega) = 0$ are identical.

Under Assumption 1, we have

$$\omega_k = \omega_h = \omega_3 = \omega_4 = \delta\sqrt{1 - 2\alpha}.$$

Hence, for $\omega < \omega_k = \omega_h,\ \varphi_k(\omega) = \varphi_h(\omega) = \pi/2$. The blue and red curves in Figure 4 are the stability switching curves and described, respectively, by

$$\left(\tau^+_{k,0}(\omega), \tau^-_{h,1}(\omega)\right) \text{ for } \omega \in [\omega_2, \omega_3]$$

and

$$\left(\tau^-_{k,0}(\omega), \tau^+_{h,1}(\omega)\right) \text{ for } \omega \in [\omega_2, \omega_3].$$

In the same way, for $\omega > \omega_k = \omega_h,\ \varphi_k(\omega) = \varphi_h(\omega) = 3\pi/2$. The green and orange curves are also the stability switching curves and described, respectively, by

$$\left(\tau^+_{k,1}(\omega), \tau^-_{h,1}(\omega)\right) \text{ for } \omega \in [\omega_4, \omega_1]$$

and

$$\left(\tau^-_{k,1}(\omega), \tau^+_{h,1}(\omega)\right) \text{ for } \omega \in [\omega_4, \omega_1].$$

As can be seen in Figure 4, these curves construct an egg-shaped closed curve. Since equations (31) and (33) indicate that m is a horizontal shift parameter and n is a vertical shift parameter, increasing the value of m shifts the closed curve rightward and increasing the value of n shifts the closed curve upward. The result obtained so far is summarized as follows:

Theorem 4 *From (31) and (33), the following pairs of delays,*

$$\left\{ \left(\tau^{\pm}_{k,m}(\omega), \tau^{\mp}_{h,n}(\omega)\right) \mid \omega \in \Omega \right\}$$

construct the set of all crossing curves on the (τ_k, τ_h) plane for equations (10).

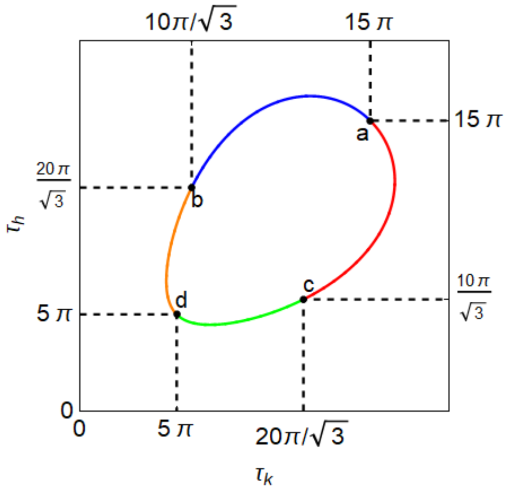

Figure 4. Crossing curve with $B_k(\omega) \neq 0$ and $\alpha = \beta$

The stability switching curve under Assumption 1 is obtained by placing Figure 3 over Figure 4 which is illustrated in Figure 5(A). It has been confirmed that the stationary point without delays is locally asymptotically stable. Hence the stability region is the region including the origin (i.e., $\tau_k = \tau_h = 0$) and surrounded by the two black, orange and green curves. The real parts of the characteristic roots are negative for τ_k and τ_h in the stability region. If a pair of the delay is selected from this region, then the steady state of the delay system (10) is locally asymptotically stable. If the pair crosses one of the boundary segments, then the real parts of one pair of characteristic roots become positive and thus the stationary state loses stability. The boundary of the stability region is called the stability switching locus. The stability region and the switching curve without Assumption 1 is also numerically illustrated in Figure 5(B) in which $\alpha = 3/10$ and $\beta = 1/3$. The stability region is surrounded by the blue, orange and green curves. It can be seen that the symmetric stability region in Figure 5(A) is distorted by the asymmetry of α and β. The dotted horizontal lines are referred in Section 5.

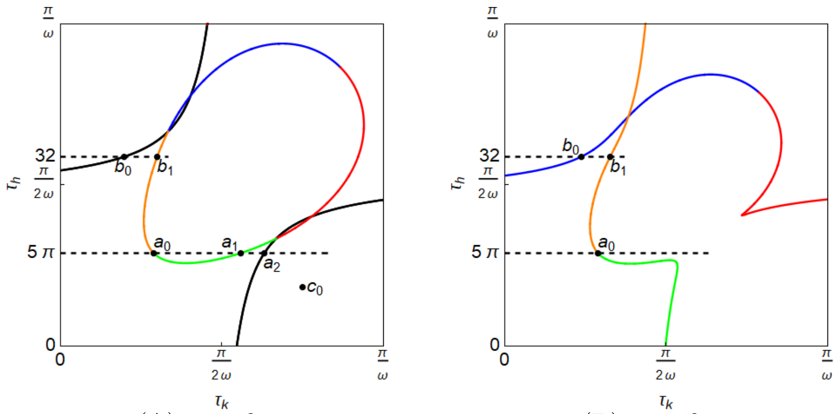

(A) $\alpha = \beta$ (B) $\alpha < \beta$

Figure 5. The stability switching curves

5 Numerical Simulations

We numerically justify the validity of the analytical results obtained in the previous sections. We mainly perform numerical simulations with the symmetric parameter values,

$$\alpha = \beta = 1/3, \ \delta = 1/10 \text{ and } s_h = s_k = 1/3$$

and the asymmetric parameters,

$$\alpha = 3/10 < \beta = 1/3, \ \delta = 1/10 \text{ and } s_h = s_k = 1/3.$$

Given initial values of physical and human capital and constant initial functions,

$$k(t) = k^* + 0.1 \text{ and } h(t) = h^* + 0.1 \text{ for } t \leq 0,$$

we run the delay system (10) for $0 \leq t \leq T$ ($T = 5,000$). k^* and h^* are the steady state given in (6). The first numerical results are given in Figure 6 in which two bifurcation diagrams are represented, one with the symmetric parameters $\alpha = \beta$ in Figure 6(A) and the other with the asymmetric parameters $\alpha < \beta$ in Figure 6(B). The value of τ_k increases along the horizontal dotted line at $\tau_h = 5\pi$ in both figures. In case of $\alpha = \beta$, the dotted line crosses the stability switching curve three times at points a_0, a_1 and a_2 where the corresponding values[4] of τ_k are

$$\tau_k^{a_0} = 5\pi \simeq 15.71, \ \tau_k^{a_1} \simeq 30.32, \ \tau_k^{a_2} \simeq 34.25.$$

[4] Returning to equation (21), we solve $\cos 5\pi\omega = M/D$ for τ_k to obtain this critical value.

It is seen that the steady state loses stability at point a_0 and replaced with oscillatory behavior. However, oscillation rapidly increases and sooner or later loses its economic meaning. When the value of τ_k gets closer to point a_1, oscillation rapidly disappears and the steady state regains stability. Further increasing the value of τ_k leads to stability loss again at $\tau_k = \tau_k^{a_2}$ and no stability regain occurs for $\tau_k > \tau_k^{a_2}$. Qualitatively different bifurcation scenario is seen in Figure 6(B) in which the stability loss takes place at point a_0 with $\tau_k^{a_0} = 5\pi$ and oscillations emerge for larger values of τ_k. If we increase the value of the delay along the diagonal in Figure 6(A), then we obtain a numerical example generated by one-delay model (10) with $\tau_k = \tau_h$. In the same way as described in Figure 6(A), the steady state of the one-delay model loses stability at point a_0 and becomes unstable for larger values of the common delay because the critical value of the delay in Theorem 3 is, under the symmetric parameters,

$$\tau_{+,0} = \frac{\pi}{2\omega_+} = 5\pi \text{ with } \omega_+ = \delta = \frac{1}{10}.$$

.

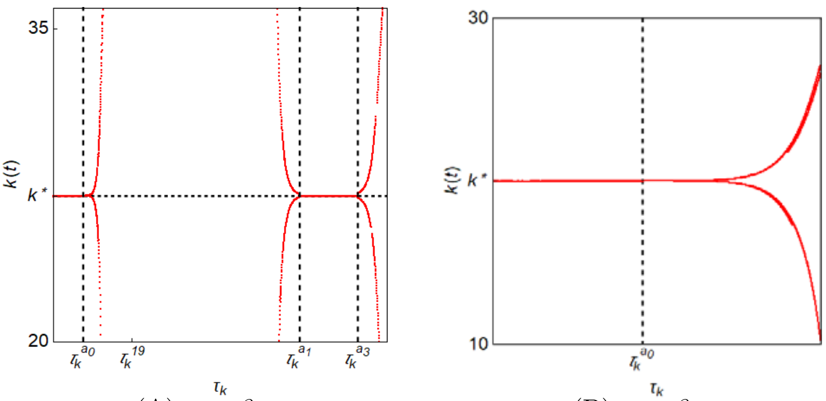

(A) $\alpha = \beta$ (B) $\alpha < \beta$

Figure 6. Bifurcation diagrams

In the second example, we examine what dynamics emerges for $\tau_k \in (\tau_k^{a_0}, \tau_k^{a_1})$ with $\tau_h = 5\pi$. For $\tau_k^{19} = 19$ in Figure 6(A), a trajectory starting in the neighborhood of the steady state is oscillatory and moves away. In consequence, either $k(t)$ or $h(t)$ might take a negative value, implying the loss of economic meaning. This is because the model has only weak nonlinearities that are not enough for preventing trajectories from being negative. One divergent example is given in Figure 7 in which the trajectory takes $h(t) \simeq 0.0097$ at $t = 1883.22$ and $h(t) \simeq -0.015$ at $t = 1883.23$. It is numerically confirmed that the delay model (10) generates infeasible global dynamics for any τ_k in the first unstable interval.

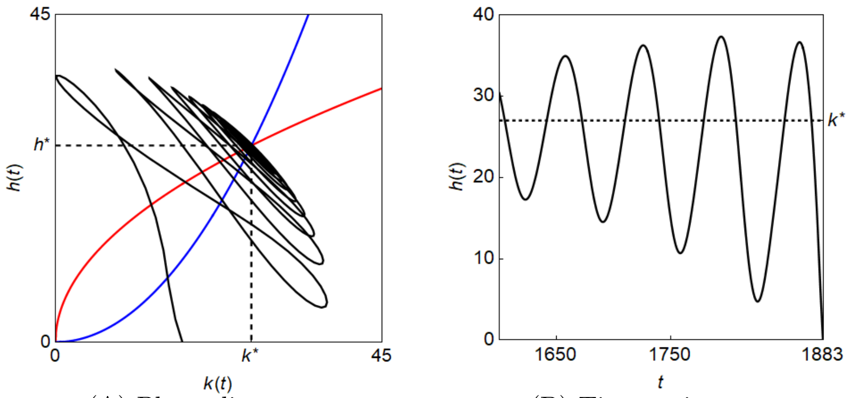

(A) Phase diagram (B) Time trajectory

Figure 7. Divergent dynamics with $\tau_k = 19$ and $\tau_h = 5\pi$

The third example concerns with the birth of a bounded limit cycle for $\tau_k > \tau_k^{a_2}$. Figure 8(A) illustrates a bifurcation diagram with respect to τ_k for $\tau_k \in (34, 42.7)$, the second unstable interval, in which the delay model gives rise to a limit cycle when the stability is lost. It is also numerically confirmed that the model generates negative dynamics for $\tau_k > 42.7$ so there is no need for further simulations. In Figure 8(B), the birth of a limit cycle is seen in the (h, k) plane when $\tau_k = 38$.

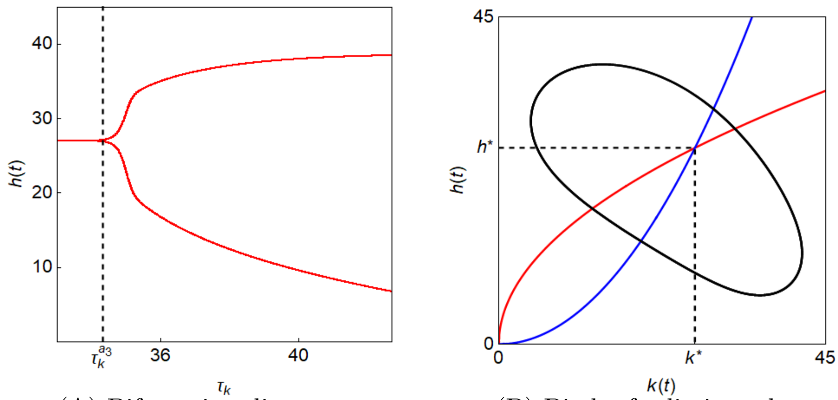

(A) Bifurcation diagram (B) Birth of a limit cycle

Figure 8. Emergence of limit cycles with $\tau_h = 5\pi$ and $\tau_k \geq \tau_k^{a_2}$

In the fourth example, the value of τ_h is increased to 32 from 5π and the value of τ_k is increased along the horizontal dotted line. The bifurcation diagrams is given in Figure 9 in which the steady state is unstable for smaller values of τ_k, gains stability at point b_0 and loses stability at point b_1. The corresponding values of τ_k are

$$\tau_k^{b_0} \simeq 10.72 \text{ and } \tau_k^{b_1} \simeq 16.29.$$

It is seen that the limit cycles for $\tau_k < \tau_k^{b_0}$ are bounded which are economically meaningful. However the limit cycles for $\tau_k > \tau_k^{b_1}$ are rapidly divergent and therefore lose economic meaning.

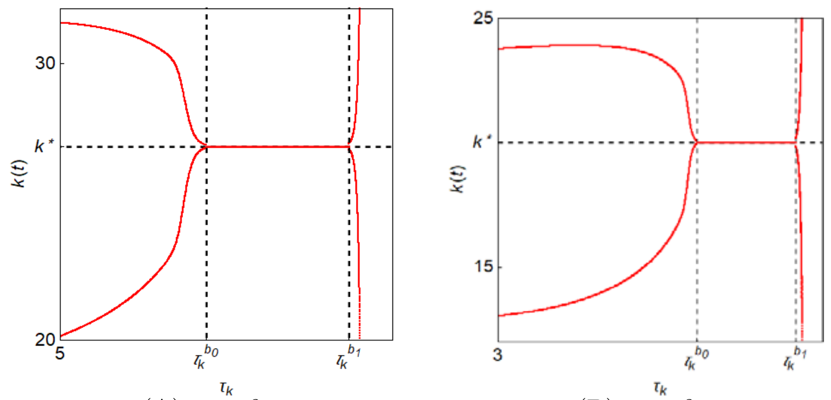

(A) $\alpha = \beta$ (B) $\alpha < \beta$

Figure 9. Bifurcation diagram along $\tau_h = 32$

The last example is illustrated in Figure 10(A) which is a part of a bifurcation diagram with respect to $\tau_k \in (38, 40.9)$ in the neighborhood of point c_0 in Figure 5, taking $\tau_h = 10$. It is seen that complicated dynamics involving chaotic oscillations emerges for larger values of τ_k.

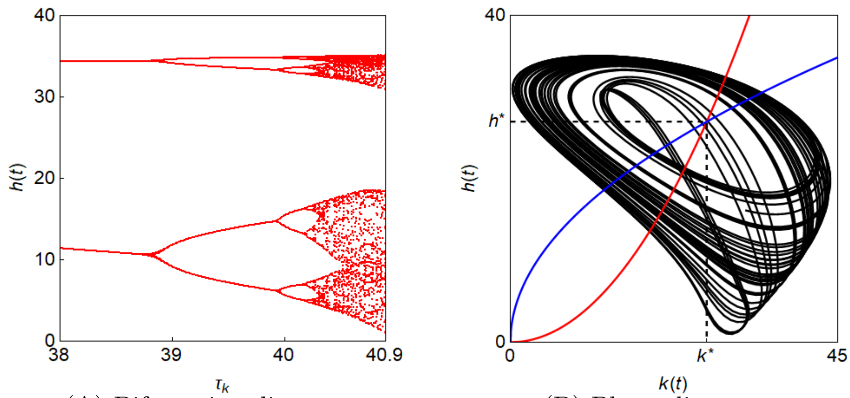

(A) Bifurcation diagram (B) Phase diagram

Figure 10. Birth of complicated dynamics; $\tau_k = 40.8$ and $\tau_h = 10$

6 Concluding Remarks

A delay extended Solow model was developed in which a Cobb-Douglas production function had three factors, physical capital, human capital and labor. Output was used for investment in physical capital as well as for human capital and consumption. A crucial element of the model was the assumption that construction of the new capitals was delayed due to a gestation time in physical capital and a maturation time in human capital. A stability switching curve on which stability is lost was analytically derived. The theoretical results were numerically confirmed and the study suggests that the delays could be source of endogenous fluctuations. One drawback of the model is that it could not prevent unstable trajectories from being negative maybe due to insufficient nonlinearities of the model.

Dinuopolos, E. and Thompson, P., Reassessing the empirical validity of the human capital augmented neoclassical growth model, Journal of Evolutionary Economics, 9, 135-154, 1999.

Domer, E., Capital expansion, rate of growth, and employment, *Econometrica*, 14, 137-147, 1946.

Goodwin, R., The nonlinear accelerator and the persistence of business cycle, *Econometrica*, 19, 1-17, 1951.

Greiner, A., Semmler, W. and Gone, G., *Economic growth: a time series perspective*, Princeton University Press, 2005.

Guerrini, L., Matsumoto, A. and Szidarovszky, F., Delay Cournot duopoly models revisited, *Chaos* 28, 093113, 2018.

Guerrini, L., Matsumoto, A. and Szidarovszky, F., Neoclassical growth model with two fixed delays, forthcoming in *Metroeconomica,* 2019.

Hall, J. and Jones, C., Why do some countries produce so much more output per worker than others?, *Quarterly Journal of Economics*, 83-115, 1999.

Harrod, R., An essay in dynamic theory, *Economic Journal*, 49, 14-33, 1939.

Jones, C., *Introduction to economic growth*, Norton, 1998.

Jones, C., Time series tests of endogenous growth models, *Quarterly Journal of Economics*, 110, 495-525, 1995.

Kaldor, N., A model of the trade cycle, *Economic Journal*, 50, 78-92, 1940.

Kalecki, M., A Macroeconomic theory of business cycle, *Econometrica*, 3, 327-344, 1935.

Klenow, P. and Rodriguez-Clare, A., The neoclassical revival in growth economics: has it gone too far? In Bernanke, B. S. and Totemberg J. J., (eds.) *NBER Macroeconomic Annual*, 73-103. MIT Press, Cambridge, MA, 1998.

Kydland, F. and Prescot, E., Time to build and aggregate fluctuations, *Econometrica*, 50, 1345-1370, 1982.

Li, X. and Wang, E., Stability analysis of delay differential equations with two discrete delays, *Canadian Applied Mathematics Quarterly*, 20, 519-532, 2012.

Mankiw, N., Romer, D. and Weil, D., A contribution to the empirics of economic growth, *Quarterly Journal of Economics*, 107(2), 407-437, 1992.

Matsumoto, A. and Szidarovszky, F., *Dynamic oligopolies with time delays*, Springer-Verlag, Tokyo, 2018.

Solow, R., A contribution to the theory of economic growth, *Quarterly Journal of Economics*, 70, 65-94, 1956.

Swan, T., Economic growth and capital accumulation, *Economic Record*, 32, 334-361, 1956.

Szydlowski, M. and Krawiec, A., A note on Kaleckian lags in the Solow model, *Review of Political Economy*, 16, 501-506, 2004.

Zak, P., Kaleckian lags in general equilibrium, *Review of Political Economy*, 11, 321-330, 1999.